

Far-Field Pattern Measurement and Simulation of VHF Antenna at 60 MHz for Europa Clipper mission

Yasser Hussein, Joshua Miller, Vachik Garkanian, Emmanuel Decrossas

Jet Propulsion Laboratory,
California Institute of Technology
4800 Oak Grove Dr.
Pasadena, CA, 91009

Yasser.Hussein@jpl.nasa.gov, Joshua.M.Miller@jpl.nasa.gov, Vachik.Garkanian@jpl.nasa.gov,
Emmanuel.Decrossas@jpl.nasa.gov

Abstract—This paper presents measurements and simulations of a linearly polarized VHF folded dipole operating at 60 MHz for NASA’s upcoming Europa Clipper mission. The spacecraft contains a ground penetrating radar, consisting of an array of four VHF antennas, that will characterize the surface of Jupiter’s icy moon Europa. Measured far-field radiation patterns and reflection coefficients above a 50×80m perfect ground plane are compared to predicted results using commercial software. Normalized Far-Field radiation pattern cuts are measured utilizing a biconical antenna and receiver mounted on a flying drone. Simulations of the radiation pattern show that the number of lobes increases with the distance of the antenna from the ground due to the ground-bounce phenomenon. In addition, the measured and simulated reflection coefficients stay unchanged for height above 2 meters, which matches the predicted calculation of the reactive-near field region of this antenna. However, the antenna electrical parameters are optimized for use on the spacecraft and become detuned in the presence of a ground plane. Simulated and measured return loss discrepancy less than 0.5 dB is presented. Radiation pattern comparisons show similar agreement when taking into account the effect of far-field measurement uncertainties.

Keywords—VHF antenna, ground penetrating radar, drone, far-field measurement, low frequency antennas, antenna pattern, Open Area Test Site (OATS), Europa Clipper, Jupiter.

I. INTRODUCTION

REASON (Radar for Europa Assessment and Sounding: Ocean to Near-surface) is a joint instrument with collaboration among NASA JPL, University of Texas Institute for Geophysics, John Hopkins APL, and the University of Iowa. The antenna design will be used in an array for radar application during several flybys to study the icy crust of Europa. The Europa REASON instrument has five science and reconnaissance objectives: 1) Characterize the distribution of any shallow subsurface water; 2) Search for an ice-ocean interface and characterize the ice shell’s global structure; 3) Investigate the process governing material exchange among the ocean, ice shell, surface, and atmosphere; 4) Constrain the amplitude and phase of gravitational tides; 5) Characterize scientifically compelling sites, and hazards, for a potential future-landing mission.

Figure 1 illustrates the proposed Europa Clipper

spacecraft, showing the folded dipole array of four antennas functioning at 60 MHz (VHF) and deployable dipole array of two antennas operating at 9 MHz (HF). This paper presents an uncommon technique to characterize these low frequency antennas on Earth. The focus of this manuscript is on accurate modeling and measurements of a single folded dipole at 60 MHz above a perfect electrical ground plane in an Open Area Test Site (OATS).

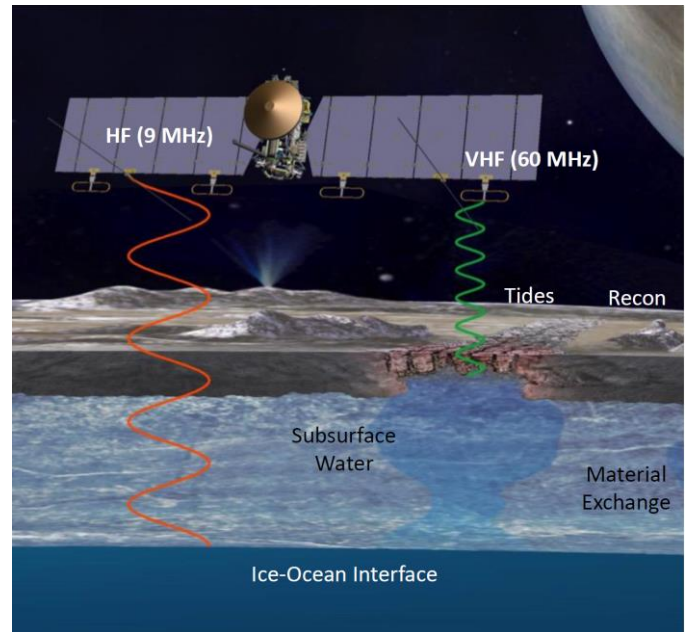


Figure 1. Illustration of the Europa Clipper spacecraft in a deployed configuration, showing the antenna placements on the solar arrays and demonstrating the five science reconnaissance objectives.

Before Selecting an OATS facility for the measurements, it is necessary to evaluate the suitability of the measurement site using inter-laboratory comparison (ILCs) and proficiency tests (PTs). ILCs are a critical activity that test houses perform in order to assure the quality of their test results. Proficiency tests (PTs) are ILCs specifically designed to evaluate participants’ performance against pre-established criteria. Various ILCs of radiated emission measurements have been proposed since the early 90’s by multinational companies such as Hewlett–Packard

(see [1]–[3]) and IBM [4]. In [3], for example, the authors reported comparison of about 33 sites across the globe. Some of these labs adopted the OATS technique, while the others adopted the use of semi-anechoic chambers. The reference site used in this paper is Keysight (formerly Liberty Calibration) in Kimballton, Iowa, USA. In [3], the authors reported relatively consistent results for frequencies greater than 30 MHz and less than 1 GHz. The site offers a 50×80m perfect electrical ground plane to conduct antenna measurements.

II. GROUND PLANE DIMENSIONS AND GROUND EFFECT

The first task was to investigate the performance of different sizes of OATS ground planes. An important part of the construction of an OATS measurement is the metallic surface laid onto the ground to stabilize the ground's reflection coefficient. Guidance on dimensions needed for the construction of an OATS and ground-plane to provide the required reflection characteristics can be found in a number of standards documents such as ANSI C63.7 [5] or EN55 022 [6]. ANSI C63.7 [5] especially analyzed the dimensions required for a good reflecting surface by exploiting the theory of Fresnel Zones.

The size and shape of the reflecting surface, or ground plane, are dependent upon the measurement geometry and whether or not the antenna can be tilted and rotated. In general, the reflecting surface is contained wholly within the obstruction-free area. It is crucial to have a flexible design and to construct the ground plane so that it can be extended in all directions. The theoretically minimum ground plane size and shape is derived from the first Fresnel elliptical zone. The first Fresnel ellipse encloses the area on the ground plane from which the major part of the ground-reflected energy comes. It is worth noting that it is important to have the capability to extend the rectangular or trapezoidal dimensions of the ground plane up to or larger than the dimensions of the Fresnel ellipse.

In [5], several ellipse dimensions for several representative measurement conditions were calculated. Table 1 summarizes some of the data. By interpolating and extrapolating, one can conclude that the test site easily incorporates the first Fresnel Zone at 60 MHz and also for the heights at which we are testing. Figure 2 depicts the dimensions provided by Table 1.

TABLE 1 FRESNEL ELLIPSE DIMENSIONS FOR SEVERAL MEASUREMENT CONDITIONS.

Measurement distance (m)	Frequency (MHz)	Antenna Heights (m)		Ellipse axes (m)	
		$h1$	$h2$	Major	Minor
R				$2XI$	$2YI$
3	30	2	4	11.3	11
3	100	2	4	7.6	7.1
10	30	2	4	16.3	13
10	100	2	4	12.4	8.1
30	30	2	4	35.2	18.9

III. PROPOSED MEASUREMENT TECHNIQUE

The VHF folded dipole prototype, as shown in Figure 3, consists of two aluminum tubes, bent and connected at the top of the antenna. A matching network at the base of the antenna is used to feed the radiating element differentially, providing the linearly polarized electrical field. The reflection coefficients of the antenna mounted vertically are measured using a network analyzer at different heights above the ground plane first from 1.25 meters up to 8 meters as shown in Figure 4. The mounting tower used for the measurement is made of fiberglass and is RF transparent at these frequencies.

The measured reflection coefficients over the 20-100 MHz bandwidth do not change when the antenna is mounted above two meters as the ground coupling effect is reduced. Experimental results show that the radiation resistance close to free space value of 72 ohms at roughly 0.45λ for a half-wave dipole [7]. This coincides with the standard equation for the far-field boundary in free space without ground, i.e. Eq. 1.

$$L < 0.62 \sqrt{\frac{D^3}{\lambda}} \quad (1)$$

This equation needs to be modified by multiplying it by 2 to account for the ground, i.e. account for the image antenna on the other side of ground while removing the ground. The new equation becomes Eq. 2.

$$L < (2)(0.62) \sqrt{\frac{D^3}{\lambda}} \quad (2)$$

When using Eq. 2, the value used for D is 2.5m, which is the maximum dimension of our antenna. For 60 MHz, this far-field boundary distance L is calculated as 2.2 meters. This value coincides with the measurements where the reflection coefficient does not vary significantly above 2.0 meters as shown in Figure 4. This is in contrast to the radiation pattern behavior, where one should expect to get more lobes as the antenna is mounted higher due to the ground bounce phenomena [7].

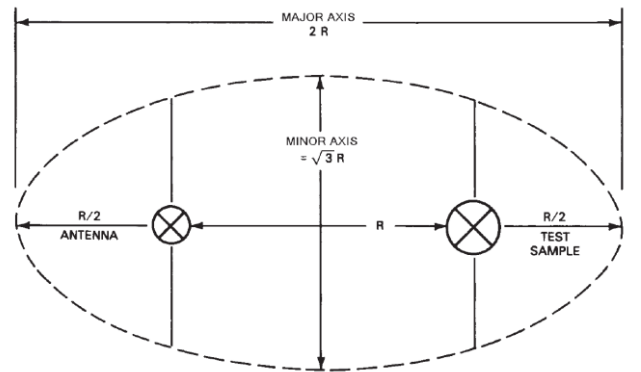


Figure 2. Fresnel zone demonstration with both antennas marked.



Figure 3. Antenna electrical team presenting the fabricated 60 MHz folded dipole prototype, about 2 meters long. From left to right: E. Decrossas, J. Miller, Y. Hussein, V. Garkanian.

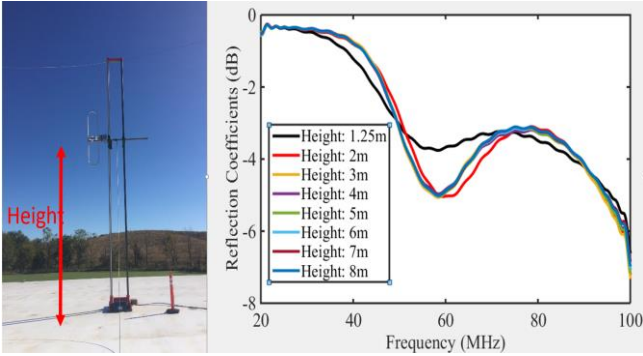


Figure 4. Measured reflection coefficient of the antenna at different height above the ground plane at the Keysight site.

Figure 5 shows a diagram of how the measured far field radiation pattern cut is performed and a picture of the drone with the mounted biconical antenna. The 60 MHz antenna is setup on the ground plane vertically and the drone is used to measure elevation pattern cuts. Repeatability error measurements are estimated by measuring the same cut several times. It is also estimated that the drone has approximately a 0.25 meter radius spherical error related to its expected location during flight using differential GPS telemetry. Differential GPS, or DGPS, uses ground based references to improve the resolution of position indication when using uncorrected GPS of approximately 15 down to 10 cm accuracy in some instances. Friis path loss equation gives approximately 0.45 dB of error at 0.25 meters. This error is calculated based on the ratio of error to wavelength of 5%. It's worth noting that polarization losses due to pitch or roll of the drone are negligible compared to its precise location error.

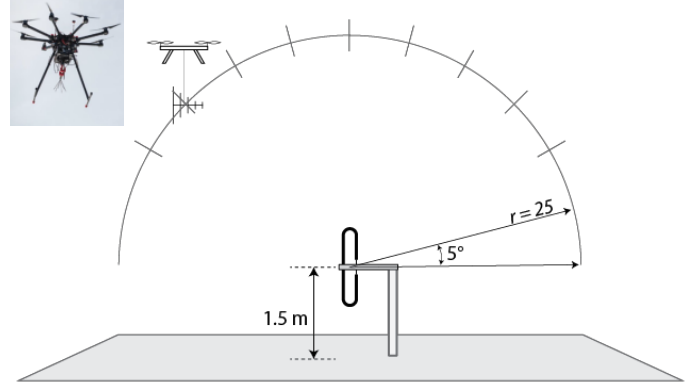


Figure 5. A diagram showing a far-field normalized pattern measurement cut. On the left is a picture of the drone with the receiver and the biconical antenna used for the measurement.

IV. GROUND-EFFECT SIMULATION AND ANALYSIS

The effect of antenna distance from ground is studied using both HFSS [8] and NEC2 [9]. In Figure 6 and Figure 7, the radiation pattern predicted by NEC2 starts to have several lobes as we go farther away from the ground plane. The number of nulls equals the distance divided by quarter wavelengths at 60 MHz, which is consistent with the ground-bounce phenomenon [7]. Simulations are carried out for a perfect ground (black curve), which is similar to our test case, and for a real ground (red curve) that considers losses such as a grass field. The simulations suggest to measure the antenna about 1.25 meters above the ground plane, from the center of the antenna, or just a few centimeters off the ground from the antenna's lower end when positioned vertically.

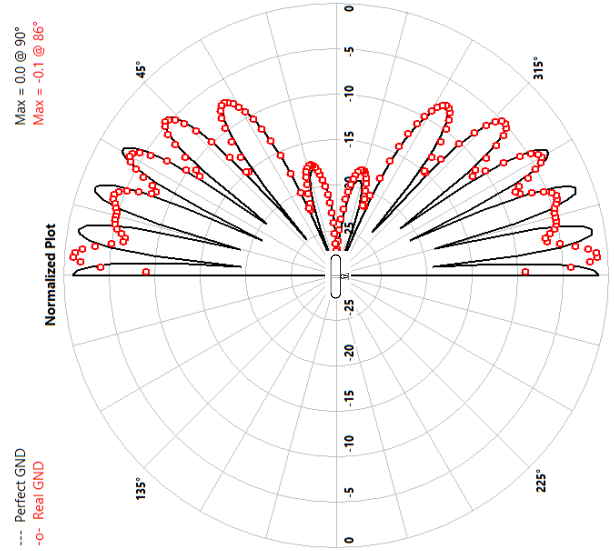


Figure 6. Simulated antenna pattern using NEC at 14.75 meters above a ground plane. In red, a lossy ground plane is considered while in black a simulated perfect ground plane is used.

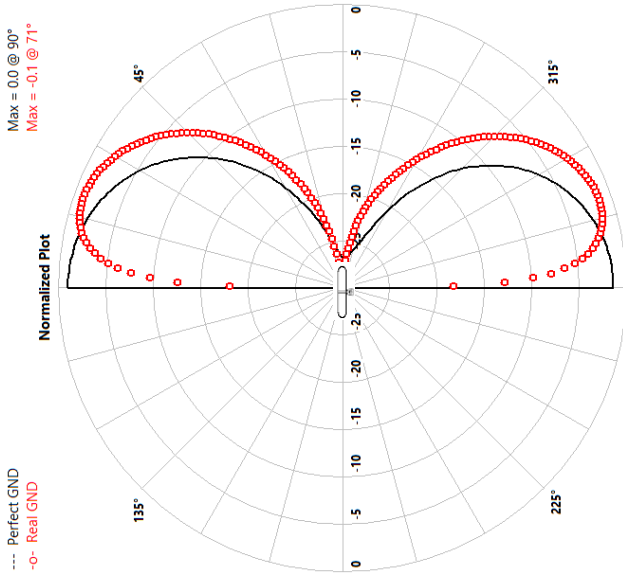


Figure 7. Simulated antenna pattern using NEC at 1.25 meter above a ground plane. In red, a lossy ground plane is considered while in black a simulated perfect ground plane is used.

V. SIMULATION AND MEASUREMENT RESULTS

A. Gain

The antenna gain is calculated using the standard site method (SSM) [10]. The antenna is scanned for distance-to-ground from 1.3 meters to 4.5 meters. The SSM measurement works by using three antennas taken in pairs. It is recommended that three antennas of the same types be used, to minimize measurements uncertainties. Measuring order is antenna 1 and 2, 1 and 3, and then 2 and 3. This creates a system of three equations with three unknowns that can then be solved. Keysight has shown repeatability accuracy of measurements using their antennas with variability < 0.1 dB using this method at this frequency. Using this approach, the proposed antenna gain was measured to be -1 dBi (± 0.1 dB). It should be noted that the antenna is tuned to be matched on the Europa spacecraft in an array configuration and is detuned from the single element measurement.

B. S-parameters

Figure 8 shows the measurements versus simulation when the center of the antenna is about 3 meters above ground. Ansys's HFSS [8] is used to calculate the complex reflection coefficient or alternatively the input impedance of the antenna, without the matching network. Then, the measured S-parameters of the matching network are cascaded with the input S-parameters of the antenna to obtain the combined reflection coefficients of the antenna. Good agreement between measurements at 3 meters above the ground (from Figure 4) and simulations are shown in Figure 8, with an estimated average error less than 0.5 dB between measured and simulated S-parameters.

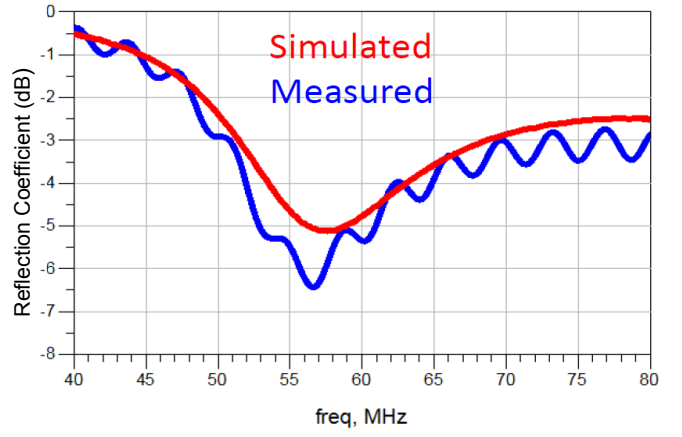


Figure 8. Measured (blue) and simulated (red) for vertically polarized dipole prototype located 3 meters above a ground plane as measured at the Keysight OATS site.

C. Radiation Patterns

The drone recorded several radiation far-field pattern measurements for different cuts. Figure 9 shows the radiation patterns for measurements and HFSS simulations for the 90° azimuthal cut. Given the measurement uncertainty and the mismatch loss in measurements, it can be concluded that good agreement is indeed confirmed from the radiation pattern curves shown in Figure 9.

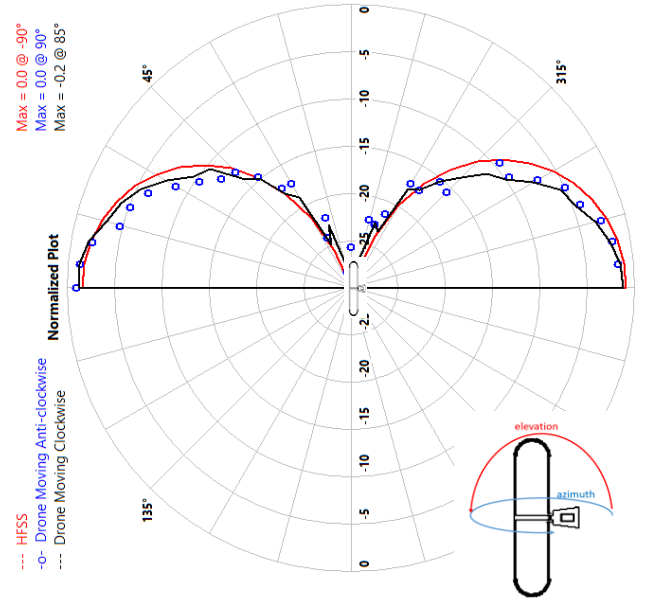


Figure 9. Normalized gain comparison among several independent measurements of the same cut to estimate the repeatability error for 90° cut. Elevation and Azimuth angle directions are shown as well.

Figure 9 shows several independent measurements comparison with HFSS: The red solid-line is when the drone moves clockwise and the blue circles are for the counter-clockwise direction. HFSS simulation data is a solid black line. For both cases, measurements match the HFSS simulations quite well, the discrepancies between measurement of the same cut independently of the drone flying direction is used to estimate the repeatability error of the system. Several radiation pattern cuts are measured and simulated at 0, 45, 135, and 270 degrees in azimuth, for all possibilities and for different drone travelling directions. All the cases show good agreement with simulation. Difference between repeated measured normalized radiation pattern is found to be less than 2 dB from 40° to 90°.

VI. SUMMARY AND FUTURE WORK

This paper presents measurements and simulations of a 60 MHz vertically polarized folded dipole antenna prototype. The final antenna design will be used in an array for radar application during several flybys to study the icy crust of Europa. The far field measurement technique using a drone is evaluated by comparing it with HFSS and NEC simulations, which match quite well. It is worth noting that what is presented in this paper is a measurement concept and its verification and validation using simulation. Other alternatives, with different tradeoffs are under investigation to characterize low frequency antennas.

VII. ACKNOWLEDGMENT

The work described in this paper was carried out at the Jet Propulsion Laboratory, California Institute of Technology, under a contract with the National Aeronautics and Space Administration. The authors would like to thank Max Dreher, Chris Gormley, Brandt Langer, Kendall Petersen, Nate Potts, and Travis Wilson from Keysight for their patience and help with our measurements.

REFERENCES

- [1] L. Kolb, "Statistical comparison of site-to-site measurement reproducibility," in *Proc. IEEE Int. Symp. Electromagn. Compat.*, Santa Clara, CA, USA, Aug. 19–23, 1996, pp. 241–244.
- [2] K. Hall, D. Pommerenke, and L. Kolb, "Comparison of site-to-site measurement reproducibility using UK National Physical Laboratory and Austrian Research Center test sites as a reference," in *Proc. IEEE Int. Symp. Electromagn. Compat.*, Washington, DC, USA, Aug. 21–25, 2000, vol. 2, pp. 939–943.
- [3] A. Crumm and K. Hall, "An update on comparison of site-to-site measurement reproducibility using HP site reference source," in *Proc. IEEE Int. Symp. Electromagn. Compat.*, Minneapolis, MN, USA, Aug. 19–23, 2002, vol. 1, pp. 35–38.
- [4] W. B. Halaberda and J. H. Rivers, "Measurement comparison of radiate test facilities measurement reproducibility using HP site reference source," in *Proc. IEEE Int. Symp. Electromagn. Compat.*, Anaheim, CA, USA, Aug. 17–21, 1992, vol. 1, pp. 401–406.
- [5] ANSI C63.7-1992 American National Standard Guide for Construction of Open Area Test Sites for Performing Radiated Emission Measurements. Published by IEEE.
- [6] BS EN55022: 1995 and CISPR 22: 1993. Limits and methods of radio disturbance characteristics of information technology equipment. British Standards Institution.
- [7] AARL, "The Antenna Book, Chapter 3: The Effects of Ground," The American Radio Relay League, Inc.; Twenty-Third Edition, Sept. 2015. ISBN 978-1-62595-044-4.
- [8] Ansoft HFSS, Pittsburgh, PA, Version 15.0.0, 2012.
- [9] NEC, Version 5.8.16, 2015.
- [10] ANSI C63.5-2006: American National Standard Electromagnetic Compatibility–Radiated Emission Measurements in Electromagnetic Interference (EMI) Control–Calibration of Antennas (9 kHz to 40 GHz)(Revision of ANSI C63)